Pol. J. Environ. Stud. Vol. 31, No. 3 (2022), 2537-2547
DOI: *10.15244/pjoes/144911* ONLINE PUBLICATION DATE: 2022-03-23

Original Research

Study on the Effect of Land-Use Change on Phosphorus Pollution In Water China, Jianjiang River, Huazhou Station Control Basin

Haitao Chen, Lijie Zheng, Wenchuan Wang*, Rui Shi

School of Water Resources, North China University of Water Resources and Electric Power, China

Received: 28 Sepember 2021
Accepted: 14 December 2021

Abstract

Different types of land use have a greater impact on phosphorus pollution in water bodies. In order to explore the impact of land-use change on phosphorus pollution in water bodies, this paper takes the Huazhou Station control basin of Jianjiang River in China as the research object. It uses the SWAT model to carry out a simulation study. Through the simulation analysis of total phosphorus pollution changes under three land-use scenarios, this paper reveals the temporal and spatial distribution of total phosphorus in watersheds under different land-use scenarios. The results show that: 1) The constructed SWAT model can better simulate and analyze the changes of runoff and total phosphorus in the study area. 2) The rainy season is the key period to control pollutants in the watershed of the study area, and agricultural land is the key area to control total phosphorus pollution in the watershed. 3) In the future land use planning of this area, it should occupy as little forest land as possible, and at the same time, reduce the output of total phosphorus from agricultural land through the adjustment of planting structure and the implementation of protective measures. This study can provide research ideas for land use and pollutant control. It can provide theoretical support for protecting and improving the water environment and water quality in the basin.

Keywords: Jianjiang River, SWAT model, land use, total phosphorus, time-space distribution

Introduction

Water resources are the basic guarantee for all human activities**.** The water resources per capita in China are only equal to the quarter of the world average. The shortage of water resources is particularly prominent [1]. With the accelerated development of society, water pollution is increasingly serious, so water pollution control is an important measure to improve water shortage in China. Sources of water pollutants can generally be divided into point source pollution and non-point source pollution. In recent years, due to the increase of environmental protection, a series of measures have been taken to prevent and control water pollution. Among them, point source pollution has the characteristics of small scope and easy centralized treatment, so the prevention and control of point source pollution has achieved good results. The non-point source pollution often involves a wide range and is difficult to implement. Therefore,

*e-mail: wangwenchuan@ncwu.edu.cn

the control effect of non-point source pollution is limited and there is still much room for improvement. Agricultural non-point source pollution is an important factor causing eutrophication of water body in many non-point source pollutions. Agricultural non-point source pollution often leads to excessive phosphorus content in water, and phosphorus is a key indicator of eutrophication [2]. Excessive phosphorus content will cause crazy growth of aquatic plants so that the dissolved oxygen in water greatly reduced, resulting in the death of aquatic animals and plants [3-4]. There is also an inseparable relationship between the conversion of land-use and agricultural non-point source pollution. For example, when crop types change, changes in crop growth cycles and fertilization methods will directly affect the changes in phosphorus concentration in the water body. [5]. And land-use patterns are not static. Moreover, the way of land-use is not static. It is affected by social development, national economic development, and many other aspects, among which human social activities are the most important factor. Land-use affects the hydrological cycle and material migration and directly determines the nature of the underlying surface of the land [6]. Therefore, study on the change of total phosphorus in the watershed from the perspective of land-use change to provide ideas for agricultural non-point source pollution.

Distributed hydrological model with physical mechanism as the most widely used watershed SWAT (Soil and Water Assessment Tool), its ability to simulate watershed pollutants has been confirmed by scholars at home and abroad [7-9]. In recent years, domestic and foreign scholars have used the SWAT model and improved SWAT model to carry out various water pollution studies. For example: calculation of non-point source pollutants in the watershed, analysis of watershed water environmental capacity, the influence of land-use change on runoff, soil nutrients, pollutants in the basin, and so on. Maryam et al. [5] took the foothills in the southeast of the United States as the research area and used the swat model to explore the impact of land-use change on phosphorus in the water. This study revealed how historical land-use changes affected the movement of phosphorus from soil to river, how rainfall increases, how to increase phosphorus loss, etc. Shi et al. [10] studied and analyzed the relationship between surface runoff changes and surface landscape types in the Luan River Basin. Conclude that the conversion of forest land to grassland and cultivated land will increase runoff. This study is of great significance to the rational planning of water resources, water environmental capacity development, and utilization. Qingrui Wang et al. [11] study on Xiangxi River Basin, Correcting and verifying seven different land-use conditions (static and dynamic), reveals the significance of long-term non-point source pollution simulations in watersheds when dynamic land-use inputs replace static inputs. This study can support the land use input conditions set when using other non-point source models in other regions.

At present, the research on pollutant phosphorus has become a hot spot [4-12-13]. However, in previous studies, most of them studied the impact of past land-use changes on runoff and pollutants, less prediction of the impact of future land-use change on total phosphorus in the watershed, and corresponding suggestions. In view of this, this paper takes the control basin of Huazhou Station in the Jianjiang River Basin as the research area, combined with the local development plan, and sets up different land-use scenarios. The swat model was used to study the influence of future land use transformation on the total phosphorus load intensity of the watershed, and suggestions were provided for future land use in the region from the perspective of total phosphorus control. This study provides research ideas for land use and pollutant control. It can also provide theoretical support for protecting and improving the water environment and water quality in the basin.

Material and Methods

Study Area

Jianjiang River is the third largest water system in Guangdong Province, originating from Wuli Mountain in Xinyi. Jianjiang River Basin is mainly located in the southwest of Guangdong Province. The basin area is 9464 km^2, of which 745 km^2 is in Guangxi. The mainstream flows from north to south through Gaozhou, Huazhou, Wuchuan and other cities, with a total length of 226 km. There are 29 tributaries of the mainstream system with rain collection areas above 100 km^2, mainly Luojiang, Caojiang, Xiaodongjiang, Qihuajiang, etc., which are mainly distributed in Maoming and Zhanjiang. The mainstream is gradually widened and flat from top to bottom. Many tributaries flow in one by one, which is prone to flooding.

Huazhou station is located in Huazhou City, and it is located 500 meters below the confluence of the tributary Luo River and the mainstream of the Jian River. The catchment area controlled by Huazhou section is more than 65 % of the whole basin (Fig. 1). The region has more people and less land, the climate is good, suitable for the growth of many crops. It is also the largest oil base in southern China.

Data Source

1) Land use data : Land use data for 2005, 2010 and 2018, with a resolution of 1 km, come from the Resource and Environmental Science Data Center of the Chinese Academy of Sciences (www.resdc.cn).

2) DEM data from CGIAR-CSISRTM (http://srtm.csi.cgiar.org), resolution is 30 m, at the same time, a series of clipping, watershed division, projection transformation and so on to get the DEM map of the study area.

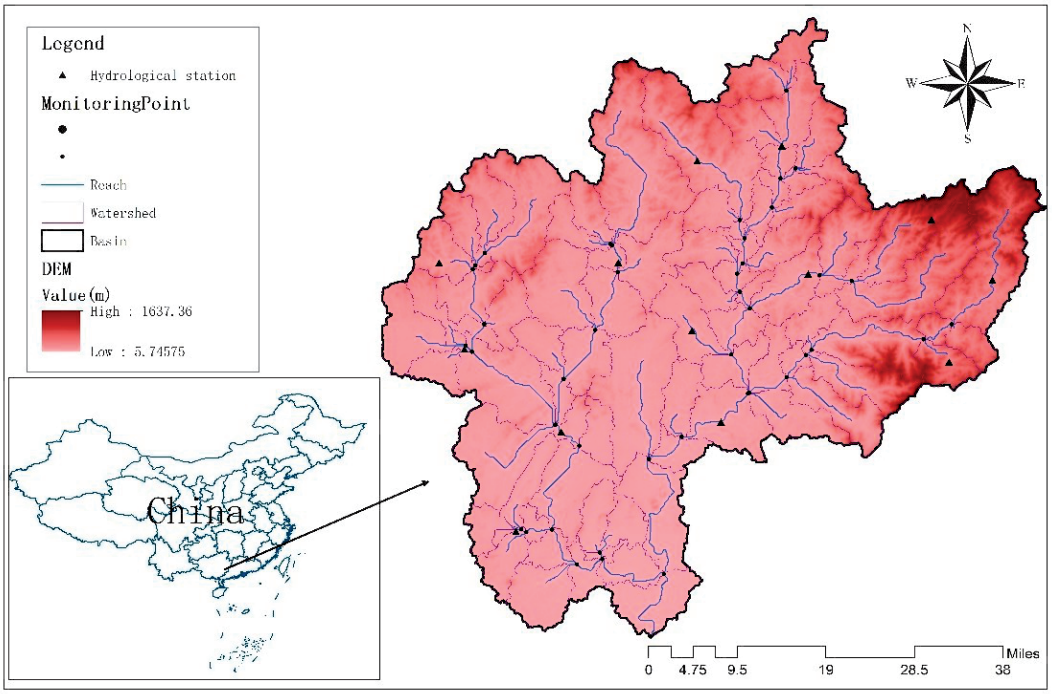

Fig. 1. Location of the study area.

3) The soil database of the study area comes from the World Soil Database (HWSD), which is divided according to the SWAT model to get the soil type of the study area, as shown in Fig. 2.

4) Refer to the local statistical yearbook for agricultural management data.

5) The rainfall data and runoff data were obtained from the local hydrological bureau. The rainfall data were from 1980 to 2018. The runoff data were read from the water resources bulletin of Guangdong Province to obtain the data from 2011 to 2019. The local hydrological bureau provided the total phosphorus data in water quality data from 2012 to 2018 (missing in 2016).

6) Temperature, humidity, wind speed, etc. are implemented with the CFSR-WORLD dataset.

All coordinate data in this study are unified as WGS_1984_World_Mercator.

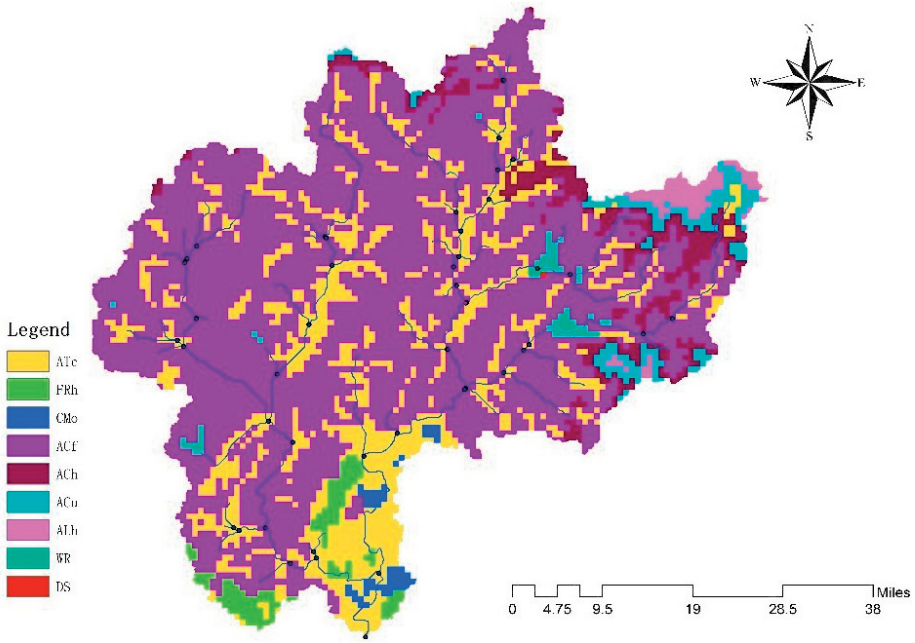

Fig . 2. Soil type map of the study area.

SWAT Model Construction

According to the DEM map of the region, the study area is set to 4000ha basin area threshold, which can be divided into 89 sub-basins. With the land use in 2010 as the background, combined with the local soil type data and the measured rainfall data, the SWAT model of the control area of Huazhou station is constructed. At the same time, the measured data of runoff and pollutants at Huazhou Hydrological Station were used, with 2010-2011 as the preheating period, 2012-2015 as the calibrated period, and 2017-2018 as the verification period (missing in 2016). The parameters of monthly runoff and total phosphorus of pollutants in the study area were calibrated to simulate the runoff and total phosphorus production in the basin.

Evaluation Criteria of the Model

The SWAT model is a continuous distributed hydrological model based on physical mechanisms [14]. It can simulate the spatial distribution characteristics of non-point source load and combine different structural analysis methods to select the best management measures to control non-point source pollution. In this study, the SUFI-2 algorithm in SWAT-CUP is used to calibrate and verify the parameters of the SWAT model. Correlation coefficient (R^2), Nash-Sutcliffe efficiency coefficient (E_{NS}), and Percentage deviation (PBIAS) are selected as the evaluation indexes of the model.

$$R^2 = \frac{\left[\sum_{i=1}^{n}(Q_i - Q_{mean})g(P_i - P_{mean})\right]^2}{\sum_{i=1}^{n}(Q_i - Q_{mean})^2 g\sum_{i=1}^{n}(P_i - P_{mean})^2} \quad (1)$$

$$E_{NS} = 1 - \frac{\sum_{i=1}^{n}(Q_i - P_i)^2}{\sum_{i=1}^{n}(Q_i - Q_{mean})^2} \quad (2)$$

$$PBIAS = \frac{\sum_{i=1}^{n}(O_i - P_i)\times 100}{\sum_{i=1}^{n} O_i} \quad (3)$$

Table 1. Sensitivity analysis of parameters.

Parameter	Description	Optimal value of parameters	Sensitivity ranking
CN2	SCS runoff curve coefficient	0.24	7
ALPHA_BF	Base flow α coefficient	0.52	21
GWQMN	Water level threshold	1015.69	22
GW_REVAP	Reevaporation coefficient of shallow groundwater	0.059	8
ESCO	Soil evaporation compensation coefficient	0.74	2
CH_N2	N Value of Manning Formula for Main River	0.041	1
CH_K2	Effective permeability coefficient	105.97	5
ALPHA_BNK	Base flow α factor for bank regulation	0.14	3
SOL_AWC	Available soil water holding capacity	0.82	6
SOL_K	Soil saturated permeability coefficient	0.38	16
SOL_BD	Soil dry volume mass	0.21	4
GW_DELAY	Time delay of groundwater	188.40	10
REVAPMN	Reevaporation water level threshold	515.85	11
SLSUBBSN	Average slope length	-0.77	9
CANMX	Maximum canopy water storage	0.16	14
PPERCO	Phosphorus permeability coefficient	12.02	18
ERORGP	Phosphorus enrichment rate	6.27	13
P_UPDIS	Phosphorus absorption distribution parameters	-9.29	17
PSP	Phosphorus availability index	0.65	12
PHOSKD	Distribution coefficient of soil phosphorus	133.09	20
SOL_ORGP	Initial concentration of soil organic phosphorus	82.00	19
EPCO	Crop consumption compensation factor	0.49	15

Table 2. Evaluation of monthly simulation results of SWAT model.

Evaluating Indicator		R^2	E_{NS}	PBIAS
Monthly Runoff	Calibration	0.72	0.72	2.7%
	Validation	0.84	0.77	12%
Monthly TP	Calibration	0.74	0.67	24.1%
	Validation	0.72	0.53	23.8%

In the formula: Q_i and Q_{mean} are measured and measured average, P_i and P_{mean} are simulated and simulated average. The closer R^2 and E_{NS} are to 1, the closer PBIAS is to 0, indicating that the simulation value is closer to the measured value. It is generally believed that R^2 is greater than 0.6, E_{NS} is greater than 0.5, and PBIAS is less than 25% [15-16].

Results and Discussion

Model Calibration and Validation

Taking the land use data in 2010 as background data, input the above-processed data in sequence to get the results, and finally use the SWAT-CUP tool to make corrections. Before the simulation, this article first conducts parameter sensitivity analysis, and then the SUFI-2 algorithm in SWAT-CUP is used to calibrate the parameters. The final parameters selected by the model are shown in Table 1.

Through 1500 iterations, the results of the model are shown in Table 2. The Correlation coefficient, Nash efficiency coefficient and Percentage deviation of calibration period all meet the accuracy requirements. Fig. 3 and Fig. 4 show the comparison between the simulated and measured values of monthly runoff and monthly total phosphorus (the data in 2016 are missing). It can be seen that the constructed SWAT model can be used to simulate runoff and total phosphorus in the study area.

Land-Use Change Analysis

The land-use transfer matrix can comprehensively summarize the structural characteristics of land use change and describe the change of transfer direction. The land-use data of 2005 and 2018 were divided into six categories, according to the classification system provided by the Resource and Environmental Science Data Center of Chinese Academy of Sciences. Two periods of land-use change can be expressed by the land-use transfer matrix, see Table 3. It can be seen from this table that the land-use change in the region decreased from the area of woodland and water area, while the construction land, agricultural land and grassland increased. The area of construction land increased most, with an increase of 16.2%, about 40.64 km^2. The area of agricultural land and grassland increased by 1.8 % and 5.6 %, respectively, about 15.21 km^2 and 9.45 km^2, water area decreased 8.7%, to approximately 11.50 km^2. Overall, the main changes in land use in the region from 2005 to 2018 were in the direction of increased construction land.

Land-Use Change Scenario Setting

According to Maoming City Master Plan (2011-2035), Maoming is a comprehensive hub city in western Guangdong, which is an important port and a petrochemical base. In the future, it is necessary

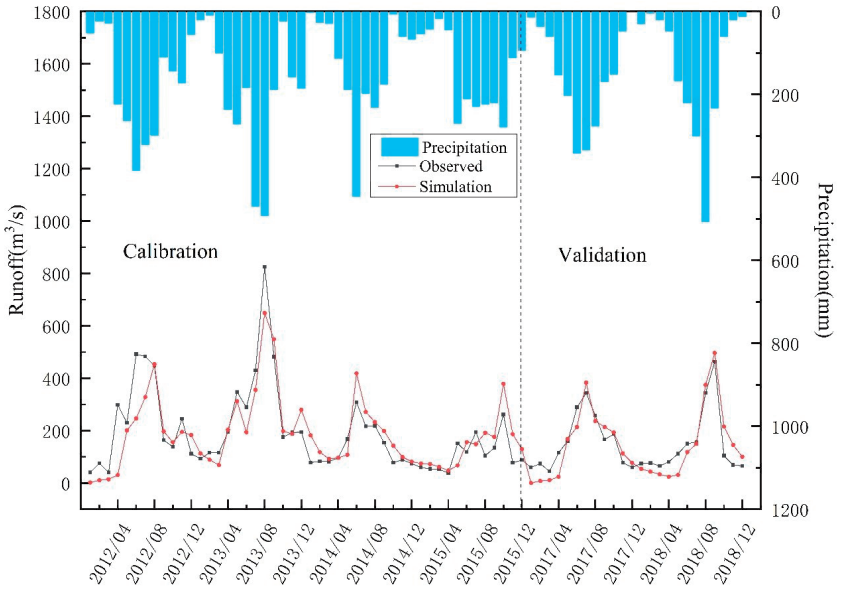

Fig. 3. Comparison of monthly runoff observed and simulated values.

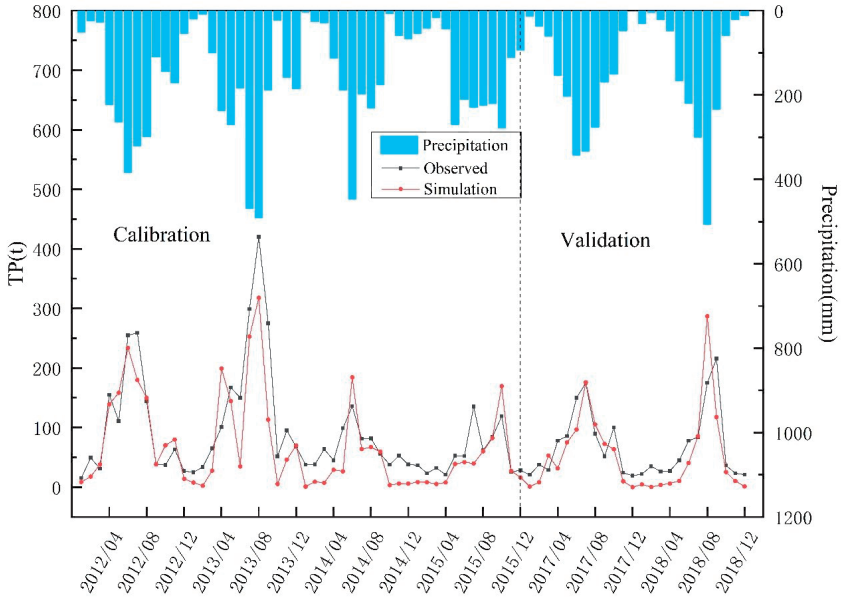

Fig. 4. Comparison of monthly TP observed and simulated values.

to improve the level of new urbanization and build this area into a world-class petrochemical base. Therefore, the region will have a large number of land types into construction land in the future. Land conversion will inevitably affect phosphorus content in water. To study the extent of the impact of the conversion of different land types, based on the land use in the study area in 2010, three land-use change scenarios were set up, study the impact of different land-use conditions on total phosphorus in the water.

Scenario 1. The scenario of sparse woodland transforming into construction land. The woodland in the study area has some nurseries, trace land and other sparse woodland with poor afforestation effect. Such land water conservation, climate regulation, reduce the effect of floods are poor. This scenario transforms the above sparse woodland and unused land into construction land. The conversion area is about 20.8 % of the initial woodland area.

Scenario 2. The scenario of transforming dry land into construction land. The agricultural land in the study area has some dry mountain land, hilly dry land, plain dry land, etc. Low production in this area, and the cost of farming is large. The scenario converted dryland and unused land into construction land, with an area of about 41.3% of the initial agricultural land.

Scenario 3. The scene of grassland transforming into construction land. There are some natural grasslands with relatively poor coverage in the study area. Such grasslands are lack of water, sparse grasslands, poor animal husbandry utilization conditions, and poor ability to protect soil erosion and wind and sand fixation. The scenario converted some low-coverage grasslands and unused land into construction land, which accounted for about 24.1 %of the initial grassland area.

Land use types under each scenario are shown in Table 4.

Table 3. Land use transfer matrix 2005-2018(km^2).

Land use type		2018 year						
		Grassland	Agricultural land	Construction land	Woodland	Water area	Unused land	Turn-out area
2005 year	Grassland	30.11	22.89	7.63	103.98	3.53	-	138.03
	Agricultural land	20.18	501.73	110.50	684.75	20.68	-	836.11
	Construction land	1.55	106.21	51.57	84.77	6.23	-	198.76
	Woodland	121.50	697.47	114.10	3436.39	57.09	-	990.16
	Water area	4.25	24.74	7.17	62.90	32.64	-	99.06
	Unused land	-	0.06	-	-	-	0.01	0.06
	Turn-in area	147.48	851.37	239.40	936.40	87.53	0	-
	Net worth	9.45	15.21	40.63	-53.76	11.50	-0.06	-

Table 4. Proportion of land use types under scenarios (%).

Land use type	Proportion of land use type area			
	Basic scenario	Scenario 1	Scenario 2	Scenario 3
Agricultural land	21.19	21.19	12.42	21.19
Woodland	70.12	55.52	70.12	70.12
Grassland	2.60	2.60	2.60	1.98
Water area	2.09	2.09	2.09	2.09
Construction land	3.98	18.6	12.77	4.62
Unused land	0.02	0	0	0

Analysis on the Influence of Land Use Change on Total Phosphorus Content

The impact of land use change on the total phosphorus content can be analyzed from two scales of time and space. The variation of the land utilization certainly affects the content of pollutants in the watershed. On the other hand, the content of total phosphorus in the watershed will also be influenced by the period and spatial distribution and will show some concomitant characteristics. Therefore, it is necessary to analyze the relationship between land-use change and the intensity of total phosphorus load from three different aspects: interannual, monthly, and spatial.

Interannual Variation of Total Phosphorus Load Intensity

Because of the above three future land use scenarios, the constructed SWAT model was used to simulate the total phosphorus content in the study area from 2012 to 2018, as shown in Fig. 5. According to the simulation results:

Under the basic scenario, the annual average load is 6842.26 t.

Under scenario 1, the load intensity of total phosphorus in the basin increased relative to the base scenario, with an average annual load of about 7094.31 t. The reason is that woodland has a strong adsorption capacity for total phosphorus of pollutants, while the construction land is relatively weak, which leads to the increase of total phosphorus load intensity in the basin, due to the change of land use in the study area.

Compared with other scenarios, the total phosphorus load intensity in scenario 2 was the lowest, with an average annual load of 4642.72 t. This scenario shows that agricultural land is an important factor in non-point source pollution, and reducing agricultural land area can effectively reduce the total phosphorus output [12].

Under scenario 3, the load intensity of total phosphorus in the basin was slightly lower than that in the basic scenario, and the annual average load was 6754.09t. It can be seen from this, the grassland adsorption capacity of pollutants is weak, but no strong woodland.

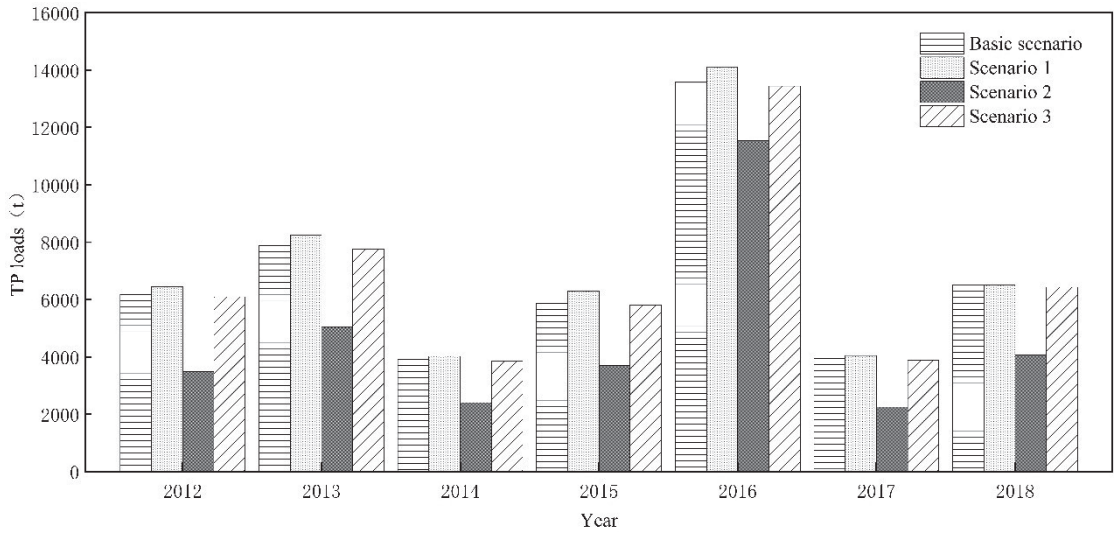

Fig. 5. Annual load intensity map of total phosphorus under different land use scenarios.

From the simulation, compared with the basic scenario, the land-use change under scenario 2 has the most significant reduction in water phosphorus pollution, and it can be seen that the largest contribution rate of phosphorus production in the study area is agricultural land, followed by grassland, the third is construction land, and the smallest contribution is woodland.

Month Variation of Total Phosphorus Load Intensity

Different land-use patterns correspond to the different state of the underlying surface of the basin, and the annual water cycle process is different, which will also have different effects on the load intensity of total phosphorus. This paper uses the established SWAT model to simulate the monthly scale of total phosphorus in three land-use scenarios and basic land-use scenarios. Using the established SWAT model to simulate the monthly scale of total phosphorus, the monthly average load intensity of total phosphorus was obtained, as shown in Fig. 6.

It can be seen from the diagram that the annual variation of total phosphorus can be divided into two stages.

The first stage is from November of the first year to March of the second year. Under the four different land-use conditions at this stage, the total phosphorus load intensity of the basin did not change significantly. The highest average total phosphorus intensity is scenario 1, which is 688.27 t, the lowest total phosphorus intensity is scenario 2, which is 578.56 t. the difference between the two scenarios is 15.9%. It shows that the load intensity of total phosphorus in the study area is not sensitive to the change of land use types. It can also be seen from the chart that the monthly load intensity of total phosphorus in January was the highest in the year. The main reason is that due to the influence of El Nino in 2016, the annual weather is abnormal, and the maximum runoff occurs in January, which leads to the highest total phosphorus intensity over the years, reaching 13576.35 t, which is the largest average in January. In addition to the impact of 2016, the annual average of total phosphorus in January under four land use conditions were 165.51 t, 171.13 t, 154.62 t, and 164.17t. There is little difference in the load intensity of total phosphorus in other months at this stage.

The second stage is from April of the second year to October of the second year. In the basic scenario, scenario 1 and scenario 3, under the three different land use conditions, the total phosphorus load intensity of the watershed has little change. The monthly average total phosphorus load intensity was 4386.56 t, 4552.59 t, and 4322.13 t, respectively. In the second scenario, the total phosphorus yield was significantly lower, and the monthly average total phosphorus load intensity was only 2457.66 t. The reason is that when this stage enters the season of crop cultivation, the amount of agricultural fertilizer increases, and this stage is the season of abundant rainfall, which is more likely to cause the loss of phosphorus in the land. As a result, scenario 2 reduced agricultural land use resulted in lower total phosphorus production.

Through the above analysis can be seen:

1) The load intensity of total phosphorus in the basin is closely related to rainfall, verifying that rainfall is the most fundamental driving factor for non-point source pollution load [17].

2) The amount of agricultural land is a key factor in phosphorus production, and its annual change is significantly affected by the tillage cycle.

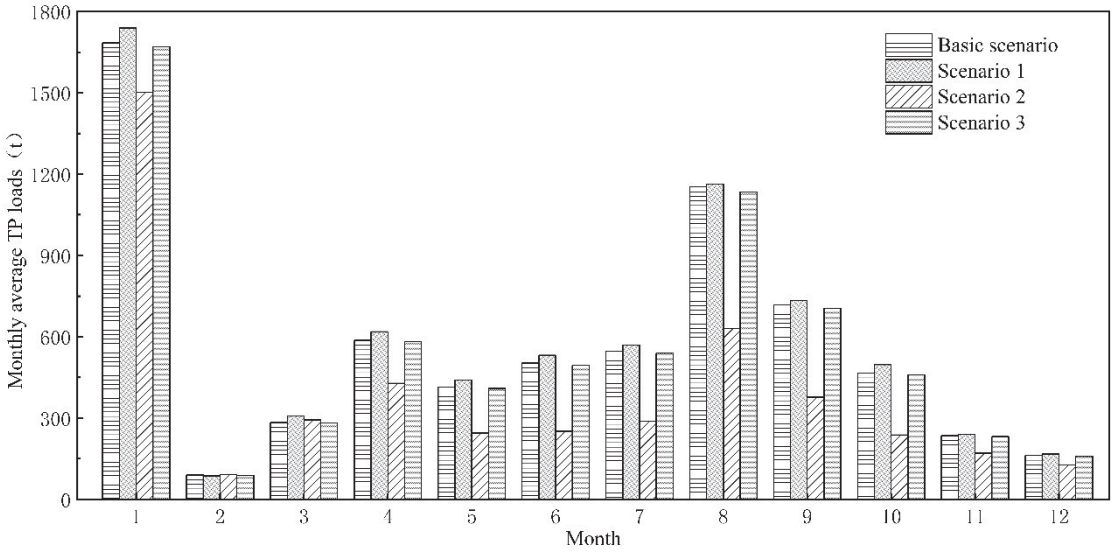

Fig. 6. Monthly average load intensity of total phosphorus under different land use scenarios.

Spatial Variation Difference of Total Phosphorus

Based on the above four different land-use scenarios, the spatial load intensity distribution map of annual average total phosphorus in each sub-basin was made, as shown in Fig. 7.

The total phosphorus load intensity under scenario 1 was slightly larger than that under basic scenario. The main reason is that more woodlands are converted into construction land in the two sub-basins 31 and 32.

The total phosphorus load intensity under scenario 2 was much lower than that under basic scenario. The main reason is that agricultural land is converted into construction land. Compared with other scenarios, the total phosphorus output of No. 61 sub-basin was significantly reduced.

The total phosphorus load intensity under scenario 3 was similar to that under basic scenario. It shows that grassland and construction land have the same effect on total phosphorus output.

In general, the sub-watersheds with higher total phosphorus loading intensity are mainly distributed in sub-basins No. 63, 69, and 73 in the southeast of the study area, and sub-basins No. 84, 85, 87, and 88 just south of the study area. These sub-basins are dominated by agricultural land.

Discussion

Influence of Extreme Weather on Model Accuracy

The SWAT model constructed in this study can better simulate the changes of runoff and total phosphorus in the basin. Still, the E_{NS} of total phosphorus is slightly lower in the verification period. This phenomenon is related to El Nino, affected by El Nino in 2016 [18], anomalous weather throughout the year, affected by the interaction of warm and humid air, non-flood season floods in the study area. The spatial and temporal distribution of rainfall is uneven during the year. The rainfall in January, March, May, August, October and November is more than that in the same period of many years. The rainfall in February, April, June, July, September, and December is less than that in the same period of many years. The maximum monthly rainfall is 399 mm in January, which is 11.2 times of the average value of the same period of many years, resulting in the maximum load of total phosphorus in this month. The emergence of abnormal maximum values often leads to the reduction of the simulation accuracy of the SWAT model and the continuity, which affects the simulation of the following year. Therefore, the E_{NS} of 2017-2018, which led to the total phosphorus in the validation period was slightly lower, but the overall simulation accuracy could still meet the requirements.

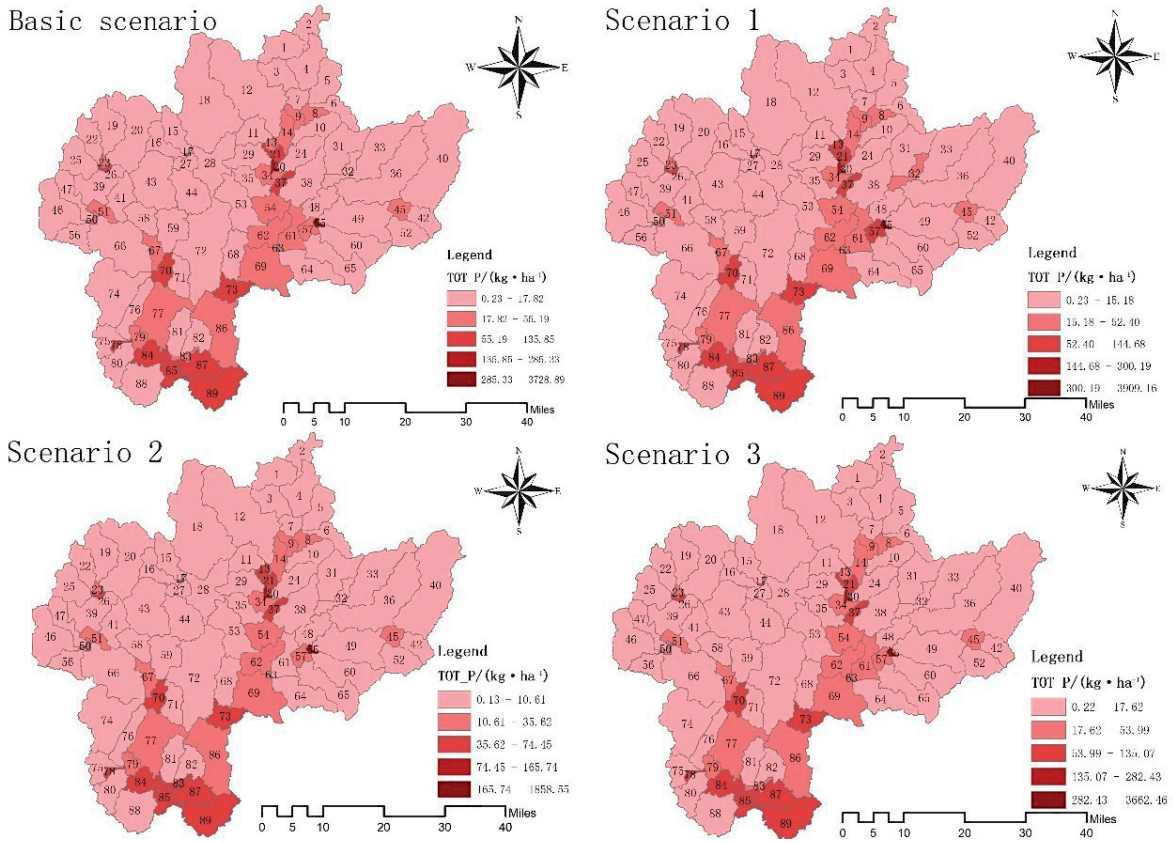

Fig .7. Load intensity of total phosphorus under different land use in sub-basins.

Effects of Different Land-Use Types on Total Phosphorus

Land-use patterns affect runoff and water quality of the basin, different land-use patterns correspond to different states of the underlying surface of the basin. The results show that: Cultivated land has the highest output intensity of total phosphorus, which is consistent with the conclusion that the average output of phosphorus pollutants is the highest on planting land [19]. The intensity of total phosphorus output from forest land is the weakest, which indicates that forests positively impact the prevention and control of pollution [20]. Previous studies have found that rainfall has a decisive impact on nutrient input in watersheds and reservoirs [21]. This study also reached the same conclusion, and the total phosphorus load was positively correlated with rainfall. Relevant studies have also reached the same conclusion [22]. The main reason is that rainfall intensity represents the erosion and dissolution ability of rainfall on soil, which is an important hydrological condition for the formation of pollutants in the basin [23].

The above conclusions show that the key area of phosphorus pollution control is agricultural land. The rainy season is the key control period of phosphorus pollution in terms of time.

Future Land Use Ideas

According to regional development planning, the increase of construction land is a trend. From the perspective of phosphorus control, this is a favorable condition. In the future land use conversion, the increase in total phosphorus output should be effectively avoided by occupying as little forest land as possible under the conditions permitted. Theoretically, converting agricultural land into construction land is conducive to the control of total phosphorus. However, the quantity of agricultural land is related to national food security and the long-term livelihood of farmers. Therefore, the occupation of agricultural land should conform to the relevant agricultural planning. In addition, the output of total phosphorus can be reduced by adjusting the planting structure of agricultural land and implementing protective measures. For example, planting some plants with high phosphorus demand in the region, such as cereals, melons and so on. This can not only effectively reduce the output of total phosphorus, but also increase crop yield and improve crop quality. It is also possible to build a buffer zone around the farmland to reduce the total phosphorus entering the water body.

Conclusions

This study took the control basin of Jianjiang Huazhou Station as the research area, set up three land use scenarios, and used the SWAT model to study the impact of different land use types on the total phosphorus load intensity. The main conclusions are as follows:

1) Extreme weather has a certain impact on the simulation results. However, the evaluation indicators of the simulation rate regular (2012-2015) and verification period (2017-2018) meet the accuracy requirements. Therefore, it is feasible to use SWAT model to conduct hydrological simulation in the study area.

2) From the perspective of land use types, cultivated land has the highest output intensity of total phosphorus, followed by construction land, and forest land has the weakest output intensity of total phosphorus. From the perspective of time period, the total phosphorus in the watershed is affected by the cycle of cultivated land, and with the increase of rainfall, the load intensity of total phosphorus in the watershed increases. Therefore, the rainy season is the key period for controlling pollutants in the watershed of the study area, and agricultural land is the key area for controlling total phosphorus pollution in the watershed.

3) The simulation analysis of total phosphorus under three different land-use scenarios shows that the load intensity of regional total phosphorus is the lowest and the impact on the environment is the lowest when cultivated land is converted into construction land. However, considering the national food security and farmers long-term livelihood, the occupation of agricultural land should be in line with the relevant agricultural planning. In future land use planning, forest land should be occupied as little as possible, and total phosphorus output should be reduced by adjusting planting structure and implementing protective measures.

Acknowledgments

The authors are grateful to Project of key science and technology of the Henan province (No: 222102320333), Henan province university scientific and technological innovation team (No: 18IRTSTHN009).

Conflict of Interest

The authors declare no conflict of interest.

References

1. WANG H., QIN D.Y., WANG J.H. Concept of system and methodology for river basin water resources programming. Journal of Hydraulic Engineering, (8), 1, **2002** [In Chinese].
2. LIU Q.P. Spatio-temoral changes of fertilization environmental risk of China. Journal of Agro-Environment Science, **36** (7), 1247, **2017** [In Chinese].
3. GUAN X.J., LIU W.K., CHEN M.Y. Study on the ecological compensation standard for river basin water

environment based on total pollutants control. Ecological Indicators, **69**, 446, **2016**.
4. HAN J., XIN Z., HAN F., XU B., WANG L., ZHANG C., ZHENG Y. Source contribution analysis of nutrient pollution in a P-rich watershed: Implications for integrated water quality management. Environ Pollut, **279**, 116885, **2021**.
5. FOROUGHI M., MALLARD J.M., NELSON D.R., SUTTER L.A., MARKEWITZ D. The impacts of historical land-use on phosphorus movement in the Calhoun Critical Zone Observatory in the southeastern US Piedmont. Biogeochemistry, **154** (1), 17, **2021**.
6. WU L., N., YANG S.T., LIU X.Y., LUO Y., ZHOU X., ZHAO H.G. Response analysis of land use change to the degree of human activities in Beiluo River basin since 1976. Acta Geographica Sinica, **69** (1), 54, **2014** [In Chinese].
7. CHEN H.T., CHEN J., LIU Y.Y., HE J. Study of Nitrogen Pollution Simulation and Management Measures on SWAT Model in Typhoon Period of Shanxi Reservoir Watershed, Zhejiang Province, China. Polish Journal of Environmental Studies, **30** (3), 2499, **2021**.
8. PEI Y.S., XU J.J., XIAO W.H., YANG M.Z., HOU B.D. Development and application of the water amount-quality and efficiency regulation model based on dualistic water cycle. Journal of Hydraulic Engineering, **51** (12), 1473, **2020** [In Chinese].
9. LIU Z., CHAO J.Y., ZHANG L., XIE Y.F., ZHUANG W., HE F. Current status and problems of non-point source pollution load calculation in China. Advances in Water Science, **26** (3), 432, **2015** [In Chinese].
10. SHI X.L., YANG Z.Y., YAN D.H., LI Y., YUAN Z. On hydrological response to land-use/cover change in Luanhe River basin. Advances in Water Science, **25** (1), 21, **2014** [In Chinese].
11. WANG Q., LIU R., MEN C., GUO L., MIAO Y. Temporal-spatial analysis of water environmental capacity based on the couple of SWAT model and differential evolution algorithm. Journal of Hydrology, **569**, 155, **2019**.
12. ZHANG L., YU Y., QIN W.G., ZHANG R. Impact of land use change on phosphorus non-point source pollution in zhuxi river basin. Journal of Hydroecology, **42** (2), 8, **2021** [In Chinese].
13. LIU L., OUYANG W., LIU H., ZHU J., FAN X., ZHANG F., MA Y., CHEN J., HAO F., LIAN Z. Drainage optimization of paddy field watershed for diffuse phosphorus pollution control and sustainable agricultural development. Agriculture, Ecosystems & Environment, **308**, **2021**.
14. RAJAT C., P. A. Effect of root zone soil moisture on the SWAT model simulation of surface and subsurface hydrological fluxes. Environmental Earth Sciences, **80** (18), **2021**.
15. CHEN Q., GOU S., QIN D.Y., ZHOU Z.H. A high efficiency auto-calibration method for SWAT model. Journal of Hydraulic Engineering, **41** (1), 113, **2010** [In Chinese].
16. QU J.H., SHI H.W., LI Z.Y. Runoff responses to climate change in Qinglong river watershed based on SWAT model. Journal of Hydroelectric Engineering, **34** (4), 8, **2015** [In Chinese].
17. GE H.F., D.Y Q., ZHOU Z.H., SANG X.F. Analysis of key source areas and pollution type in the lower Haihe River based on pollution loading movement and transformation. Journal of Hydraulic Engineering, **42** (1), 61, **2011** [In Chinese]
18. ZHANG Y.Y. Water In flow analysis of Jianjiang river basin during dry season. Guangdong Water Resources and Hydropower, (5), 38, **2020** [In Chinese].
19. XU Q.L., YANG K., LI J., YANG Y.L. Agent-based modeling of land use change and simulation of response on nonpoint source pollution for Erhai Lake watershed. Journal of Hydraulic Engineering, **45** (11), 1272, **2014** [In Chinese].
20. SONG L.L., HAO Q.Q., WANG W.H. Non point source pollution in Fuxin river basin investigated using the SWAT model. Journal of Irrigation and Drainage, **37** (4), 94, **2018**. [In Chinese].
21. DA W.Y., LI Y.X., ZHU G.W., XU H., LIU M.L., LAN J., WANG Y.C., WU Z.X., ZHENG W.T. Influence of hydrometeorological processes on nutrient dynamics in Qiandao Lake. Journal of Hydroecology, **40** (5), 9, **2019** [In Chinese].
22. GAO R., HAN H.H., CUI Y.L., WANG S.P., HUANG Y., ZHANG L. Effect of precipitation on wet deposition flux and content of nitrogen and phosphorus in Erhai lake basin in rice season. Transactions of the Chinese Society of Agricultural Engineering, **34** (22), 191, **2018** [In Chinese].
23. WANG A.J., DING W.F., WANG W.J. Characteristics of runoff and sediment yield of purple soil slope surface in the presence of artificial rainfall and scouring. Journal of Yangtze River Scientific Research Institute, **32** (3), 31, **2015** [In Chinese].